Journal of Applied Mechanics and Technical Physics, Vol. 50, No. 3, pp. 459–465, 2009

NUMERICAL MODELING OF A TURBULENT FLOW BEHIND A HEATED GRID

M. K. Baev and G. G. Chernykh

UDC 532.517.4

A numerical model of the dynamics of turbulence and temperature fluctuations behind a heated grid located in a wind tunnel is constructed on the basis of closed Kármán–Howarth and Corrsin equations. Results calculated by this model are in reasonable agreement with available experimental data.

Key words: *Kármán–Howarth and Corrsin equations, turbulence behind a grid, isotropic turbulence, turbulent fluctuations of temperature, numerical modeling.*

Introduction. Turbulence behind a grid in a wind tunnel or in a water channel is an important object of research in experimental, theoretical, and computational hydrodynamics. A detailed review of publications on this topic can be found in [1–4].

Turbulence behind a grid in a wind tunnel is known to be close to isotropic [1]. The most detailed data on turbulence degeneration behind a non-heated grid were obtained in experiments [2] where a high degree of flow isotropy was reached by means of flow contraction. Detailed experimental verification of the validity of the non-closed Kármán–Howarth equation was performed [1].

A fairly large number of models used to close the Kármán–Howarth equation in the spectral formulation are available at the moment [1]. Mathematical models based on direct closure of the Kármán–Howarth equation and written in terms of correlation functions are constructed (see [3, 4]). Among models of this type, the gradient model proposed by Lytkin [5, 6] should be noted (a similar model was later proposed in [7]). This model corresponds to Kolmogorov's hypotheses about the local isotropy of the flow [1]. Results calculated by the gradient model are in good agreement with available experimental data [2–6]. Onufriev [8] constructed a mathematical model of the dynamics of isotropic turbulence based on differential transport equations of two-point longitudinal correlation functions of the second and third orders. The model proposed in [5, 6] is a consequence of algebraic truncation of the model developed in [8]. The paper of Domaradzki and Mellor [9] should also be noted among the papers dealing with numerical modeling of the dynamics of isotropic turbulence with the use of the closed Kármán–Howarth equation. They performed an extensive study, but the closure they proposed does not describe the asymptotic behavior of the third-order longitudinal structural function of the velocity field $D_{LL,L}$ in the domain of small scales corresponding to the first Kolmogorov's hypothesis of similarity [1] (this fact was noted in [2, 4, 7, 9]). Other methods of mathematical modeling of isotropic turbulence, in particular, those based on direct numerical integration of Navier–Stokes equations, were briefly reviewed in [3, 4].

A turbulent flow behind a heated grid in a wind tunnel was also considered in some papers (see, e.g., [1, 10–12]). The main grid generating close-to-isotropic turbulence in [12] was not heated, as well as in [10]. A screen composed of wires heated by electric current was placed in an immediate vicinity of the grid to ensure heat supply to the flow. As far as the authors of the present paper are aware, the most complete results were obtained in experiments [10] where close-to-isotropic fluctuating characteristics of velocity and temperature fields were measured as functions of the distance from the grid. In particular, detailed data on the dynamics of the second-order two-point correlation functions were reported in [10].

Novosibirsk State University, Novosibirsk 630090; Institute of Computational Technologies, Siberian Division, Russian Academy of Sciences, Novosibirsk 630090; maxaus@bk.ru; chernykh@ict.nsc.ru. Translated from Prikladnaya Mekhanika i Tekhnicheskaya Fizika, Vol. 50, No. 3, pp. 118–126, May–June, 2009. Original article submitted December 20, 2007; revision submitted February 14, 2008.

0021-8944/09/5003-0459 © 2009 Springer Science + Business Media, Inc.

The results of the analysis of available publications dealing with a turbulent flow behind a heated grid allow us to conclude that numerical modeling of the flow on the basis of a close system of the Kármán–Howarth and Corrsin equations [1] was not performed. In the present paper, the Corrsin equation is closed with a gradient hypothesis similar to that proposed in [5, 6]. A numerical model of a turbulent flow behind a heated grid based on a system of closed Kármán–Howarth and Corrsin equations is constructed. The calculated results are compared with experimental data [10].

1. Formulation of the Problem. An isotropic turbulent flow and temperature fluctuations in this flow are described by the Kármán–Howarth and Corrsin equations [1, 10]

$$\frac{\partial B_{LL}}{\partial t} = \frac{1}{r^4}\,\frac{\partial}{\partial r}\,r^4\Big(B_{LL,L} + 2\nu\,\frac{\partial B_{LL}}{\partial r}\Big); \tag{1}$$

$$\frac{\partial B_{\theta\theta}}{\partial t} = \frac{2}{r^2}\,\frac{\partial}{\partial r}\,r^2\Big(B_{L\theta,\theta} + \chi\,\frac{\partial B_{\theta\theta}}{\partial r}\Big). \tag{2}$$

Here B_{LL} and $B_{LL,L}$ are the longitudinal two-point correlation functions of the velocity field of the second and third order, $B_{\theta\theta}$ is the two-point correlation function of the temperature field, $B_{L\theta,\theta}$ is the mixed third-order moment, and ν and χ are the coefficients of kinematic viscosity and thermal diffusivity, respectively.

System (1), (2) is not closed. To close Eq. (1), we use a known hypothesis of the gradient type [5, 6]

$$B_{LL,L} = 2K_1\,\frac{\partial B_{LL}}{\partial r}, \tag{3}$$

where $K_1 = \varkappa_1 r\sqrt{2[B_{LL}(0,t) - B_{LL}(r,t)]}$ is the coefficient of turbulent viscosity ($\varkappa_1$ is an empirical constant). Equation (2) is closed by a similar gradient relation

$$B_{L\theta,\theta} = K_2\,\frac{\partial B_{\theta\theta}}{\partial r}, \qquad K_2 = \varkappa_2 r\sqrt{2[B_{LL}(0,t) - B_{LL}(r,t)]}. \tag{4}$$

The value of $\varkappa_1$ was chosen to be 0.0764 [5, 6] with allowance for the fact that the Kolmogorov relation is valid in the inertial-convective interval of scales [1]:

$$D_{LL} = 2[B_{LL}(0,t) - B_{LL}(r,t)] = (1/5\varkappa_1)^{2/3}(\varepsilon r)^{2/3} = C_u(\varepsilon r)^{2/3}.$$

Here $\varepsilon = -(3/2)\,du^2/dt$ is the rate of dissipation of turbulent energy to heat, $u = \sqrt{B_{LL}(0,t)}$, and $C_u = 1.9$ is the universal Kolmogorov constant [1]. A similar analysis of Eq. (4) leads (on the inertial-convective interval of scales) to the Obukhov relation [1]

$$D_{\theta\theta} = 2[B_{\theta\theta}(0,t) - B_{\theta\theta}(r,t)] = \frac{1}{\varkappa_2\sqrt{C_u}}\,N\varepsilon^{-1/3}r^{2/3} = C_\theta N\varepsilon^{-1/3}r^{2/3},$$

where $N = -(1/2)\,d\theta^2/dt$ is the rate of equalization of temperature inhomogeneities, $\theta = \sqrt{B_{\theta\theta}(0,t)}$, and C_θ is a constant (analog of C_u). It was noted in [1] that there is a significant scatter in results of experiments performed: $C_\theta = 1.1$–6.5 (even $C_\theta = 9$ was obtained in processing of experimental data for the near-water atmospheric layer above the sea was obtained). The value recommended in [1] is $C_\theta = 3$.

Thus, for a flow with rather high values of the turbulent Reynolds and Peclet numbers, we have $\varkappa_2 = 0.112$–0.660. In the present work, the value $\varkappa_2 = 0.095$ was chosen to match the calculated and experimental data [10]. Now some publications are available (see, e.g., [8, 13, 14]), where the dependence of the turbulent viscosity coefficient in Eq. (3) on the turbulent Reynolds number is taken into account. In the present paper, however, we consider only the simplest relations (3) and (4).

As was noted in Introduction, close-to-isotropic turbulence can be provided under laboratory conditions by placing a turbulizing grid in the test section of a wind tunnel or a water channel. The measured correlation functions in the flow behind the turbulizing grids can be used for comparisons with the calculated results. It is reasonable to write Eqs. (1), (2) in the dimensionless form:

$$\frac{\partial \tilde B_{LL}}{\partial \tilde t} = \frac{2}{\tilde r^4}\,\frac{\partial}{\partial \tilde r}\,\tilde r^4\Big(\tilde K_1 + \frac{1}{\mathrm{Re}_M}\Big)\frac{\partial \tilde B_{LL}}{\partial \tilde r}; \tag{5}$$

$$\frac{\partial \tilde B_{\theta\theta}}{\partial \tilde t} = \frac{2}{\tilde r^2}\,\frac{\partial}{\partial \tilde r}\,\tilde r^2\Big(\tilde K_2 + \frac{1}{\mathrm{Pe}_M}\Big)\frac{\partial \tilde B_{\theta\theta}}{\partial \tilde r}. \tag{6}$$

Here $\tilde{B}_{LL} = B_{LL}/U_\infty^2$, $\tilde{t} = x/M$, $\tilde{r} = r/M$, $\tilde{K}_1 = K_1/(MU_\infty)$, $\mathrm{Re}_M = U_\infty M/\nu$, $\tilde{B}_{\theta\theta} = B_{\theta\theta}/\Theta^2$, $\tilde{K}_2 = K_2/(MU_\infty)$, $\mathrm{Pe}_M = U_\infty M/\chi = \mathrm{Re}_M \mathrm{Pr}$, x is the distance from the grid, U_∞ and Θ are the flow velocity and temperature in the test section of the wind tunnel or water channel, M is the cell size of the turbulizing grid, Re_M and Pe_M are the Reynolds and Peclet numbers, and $\mathrm{Pr} = \nu/\chi$ is the Prandtl number.

System (5), (6) is supplemented by the boundary conditions

$$\tilde{r} = 0: \quad \frac{\partial \tilde{B}_{LL}}{\partial \tilde{r}} = \frac{\partial \tilde{B}_{\theta\theta}}{\partial \tilde{r}} = 0, \qquad \tilde{r} \to \infty: \quad \tilde{B}_{LL} \to 0, \quad \tilde{B}_{\theta\theta} \to 0 \tag{7}$$

and the initial conditions

$$\tilde{B}_{LL}(\tilde{r}, \tilde{t}_0) = \varphi_1(\tilde{r}), \qquad \tilde{B}_{\theta\theta}(\tilde{r}, \tilde{t}_0) = \varphi_2(\tilde{r}). \tag{8}$$

In accordance with the physical meaning of the problem, the functions $\varphi_1(\tilde{r})$ and $\varphi_2(\tilde{r})$ should be continuous and bounded, have a maximum at $\tilde{r} = 0$, and tend to zero as $\tilde{r} \to \infty$.

Under the assumption of a rather rapid decrease of the functions $\varphi_1(\tilde{r})$ and $\varphi_2(\tilde{r})$ and the solution $\tilde{B}_{LL}$, $\tilde{B}_{\theta\theta}$ of problem (5)–(8) as $\tilde{r} \to \infty$, Eqs. (5), (6) yield the known Loitsyanskii and Corrsin invariants [1]:

$$\int_0^\infty \tilde{B}_{LL}\tilde{r}^4\, d\tilde{r} = \tilde{\Lambda}(\tilde{t}) = \mathrm{const} = \tilde{\Lambda}(\tilde{t}_0), \qquad \int_0^\infty \tilde{B}_{\theta\theta}\tilde{r}^2\, d\tilde{r} = \tilde{K}(\tilde{t}) = \mathrm{const} = \tilde{K}(\tilde{t}_0).$$

In what follows, the tilde is omitted.

2. Calculation Algorithm. Problem (5)–(8) was solved numerically with the use of implicit conservative difference schemes based on the integrointerpolation method [15] (see also [6]):

$$\frac{(B_{LL})_i^{n+1,s+1} - (B_{LL})_i^n}{\tau_n} = \frac{2}{r_i^4 \bar{h}_{i-1}}\Big(P_{i+1/2}^{n+1,s} \frac{(B_{LL})_{i+1}^{n+1,s+1} - (B_{LL})_i^{n+1,s+1}}{h_i}$$

$$- P_{i-1/2}^{n+1,s} \frac{(B_{LL})_i^{n+1,s+1} - (B_{LL})_{i-1}^{n+1,s+1}}{h_{i-1}}\Big); \tag{9}$$

$$\frac{(B_{\theta\theta})_i^{n+1} - (B_{\theta\theta})_i^n}{\tau_n} = \frac{2}{r_i^2 \bar{h}_{i-1}}\Big(H_{i+1/2}^{n+1} \frac{(B_{\theta\theta})_{i+1}^{n+1} - (B_{\theta\theta})_i^{n+1}}{h_i} - H_{i-1/2}^{n+1} \frac{(B_{\theta\theta})_i^{n+1} - (B_{\theta\theta})_{i-1}^{n+1}}{h_{i-1}}\Big). \tag{10}$$

Here $P = r^4(1/\mathrm{Re}_M + K_1)$, $H = r^2(1/\mathrm{Pe}_M + K_2)$, n is the number of the time layer, τ_n and h_i ($n = 0, 1, \ldots, N$; $i = 0, 1, \ldots, I$) are the steps of the difference grid over the space and time variables, respectively, $\bar{h}_i = 0.5(h_i + h_{i+1})$, $r_i = r_{i-1} + h_i$, s is the number of the iteration in terms of nonlinearity, $P_i^{n+1} = P(r_i, t_{n+1})$, $H_i^{n+1} = H(r_i, t_{n+1})$, $P_{i\pm1/2} = 0.5(P_i + P_{i\pm1})$, $H_{i\pm1/2} = 0.5(H_i + H_{i\pm1})$, and $t_{n+1} = t_n + \tau_n$.

In accordance with the boundary and initial conditions (7) and (8), the following initial-boundary conditions were imposed in solving the finite-difference problem:

$$(B_{LL})_i^0 = \varphi_1(r_i), \qquad (B_{\theta\theta})_i^0 = \varphi_2(r_i); \tag{11}$$

$$(B_{LL})_0^{n+1,s+1} = (B_{LL})_1^{n+1,s+1}, \quad (B_{\theta\theta})_0^{n+1} = (B_{\theta\theta})_1^{n+1}, \quad (B_{LL})_I^{n+1,s+1} = (B_{\theta\theta})_I^{n+1} = 0. \tag{12}$$

The value of r_I was chosen to be sufficiently large. When iterations in terms of nonlinearity were performed, it was assumed that $(B_{LL})_i^{n+1,0} \equiv (B_{LL})_i^n$. Iterations in terms of nonlinearity were performed until the condition $\max\limits_i |(B_{LL})_i^{n+1,s+1} - (B_{LL})_i^{n+1,s}| \leqslant \delta \max\limits_i (B_{LL})_i^{n+1,s}$ was satisfied, where the value $\delta > 0$ was chosen in the interval $\delta = 10^{-5}$–10^{-4} (a further decrease in δ did not yield any significant changes in the solution). Such a level of accuracy could be reached after 3–5 iterations in terms of nonlinearity [see Eq. (9)] at each time layer. The parameters τ_n, h_i, I, and δ were chosen in the course of the numerical experiments performed.

The numerical model was tested on a problem of turbulence degeneration behind a non-heated grid [2]. Experimental data were set as the initial conditions at $t_0 = 40$. The calculated and experimental dependences of $B_{LL}(0, t)$ on the distance from the grid are plotted in Fig. 1. The calculated normalized correlation function $f(r) = B_{LL}(r, t)/B_{LL}(0, t)$ at $t = 200$ is compared with the measured data (Fig. 2). It is seen that the calculated results are in good agreement with the experimental data (a detailed comparison was performed earlier in [2, 4]).

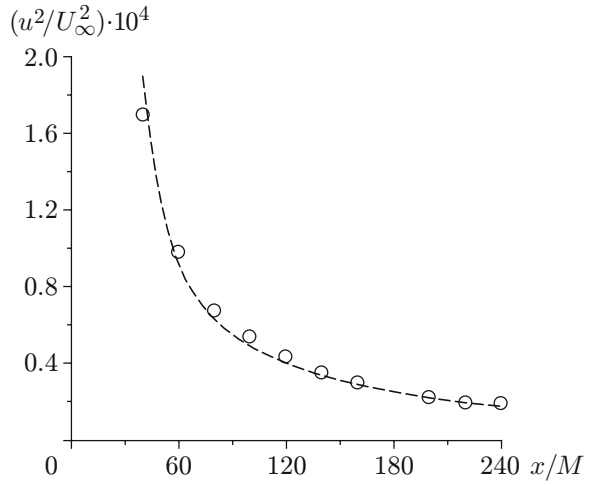

Fig. 1

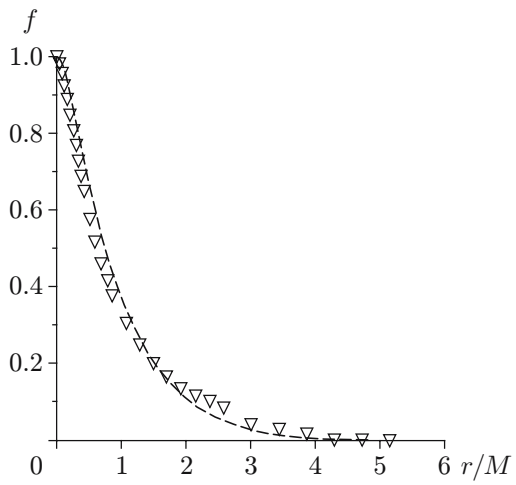

Fig. 2

Fig. 1. Quantity $u^2 = B_{LL}(0,t)$ versus the distance from the grid: the points and curve are the experimental and calculated results, respectively.

Fig. 2. Calculated and experimental normalized correlation functions $f(r) = B_{LL}(r,t)/B_{LL}(0,t)$ at $t = x/M = 200$: the points and curve are the experimental and calculated results, respectively.

The calculations were performed on a grid with $\tau_n = 0.1$, $h_0 = 5\cdot 10^{-5}$, $h_i = 1.1h_{i-1}$ $(i = 1,\ldots,91)$, and $h_i = 0.15$ $(i = 92,\ldots,350)$. To check the calculation accuracy, we also performed a calculation with the parameters $\tau = \tau_n/2$, $h_{10} = h_0/2$, $h_{1i} = 1.1h_{1i-1}$ $(i = 1,\ldots,84)$, and $h_{1i} = 0.075$ $(i = 85,\ldots,600)$. The difference between the resultant solutions was smaller than 0.8% in a uniform grid norm.

3. Calculation Results. Wind-tunnel experiments [10] included fairly detailed measurements of turbulence characteristics behind a heated grid at $\mathrm{Re}_M = 7200$ and $\mathrm{Pe}_M = 5184$. For comparisons with results calculated by the mathematical model described above, we performed a numerical solution of the system of difference equations (9) and (10) with the initial and boundary conditions (11) and (12). The correlation functions B_{LL}/U_∞^2 and $B_{\theta\theta}/\Theta^2$ obtained in [10] were used as the initial conditions at $t = x/M = 17$. The behavior of the quantities $u/U_\infty = \sqrt{B_{LL}(0,t)}/U_\infty$ and $\theta = \sqrt{B_{\theta\theta}(0,t)}/\Theta$ with increasing $t = x/M$ is illustrated in Fig. 3. It is seen that the calculated results are in good agreement with the experimental data. A significant deviation of the calculated results from the experimental data is observed at $\varkappa_2 = 0.125$ (which corresponds to $C_\theta = 5.8$ [1]).

It is known that a turbulent flow behind a heated grid is characterized by two microscales: λ_f and λ_θ [1, 10]. Each of them can be found by two methods. By definition, the Taylor microscale λ_{1f} and Corrsin microscale $\lambda_{1\theta}$ are found from the relations [1, 10]

$$\frac{1}{\lambda_{1f}^2} = -\frac{1}{2}\Big(\frac{\partial^2 f}{\partial r^2}\Big)\Big|_{r=0}, \qquad \frac{1}{\lambda_{1\theta}^2} = -\frac{1}{2}\Big(\frac{\partial^2 m}{\partial r^2}\Big)\Big|_{r=0}, \qquad m(r) = \frac{B_{\theta\theta}(r,t)}{B_{\theta\theta}(0,t)}. \tag{13}$$

Mills et al. [10] also used the relations

$$\frac{du^2}{dt} = -20\,\frac{1}{\mathrm{Re}_M}\,\frac{u^2}{\lambda_{2f}^2}, \qquad \frac{d\theta^2}{dt} = -12\,\frac{1}{\mathrm{Pe}_M}\,\frac{\theta^2}{\lambda_{2\theta}^2}, \tag{14}$$

which follow from decomposition of all terms of Eqs. (1) and (2) into the Taylor series. According to the terminology used in [1], these relations are zero terms of the expansion at $r = 0$. Relations (13) and (14) are used in [10] as independent relations. We can expect the values of λ_{1f} and λ_{2f} to be close to each other. These values coincide only for parabolic (at small values of r) correlation functions $f(r) = 1 - r^2/\lambda_f^2$. The results measured in [10] are fairly close. The results of numerical modeling almost coincide (Fig. 4a). A similar situation is observed for the experimentally obtained values of $\lambda_{1\theta}$ and $\lambda_{2\theta}$. The calculated values of $\lambda_{1\theta}$ and $\lambda_{2\theta}$ differ insignificantly (Fig. 4b).

It should be noted that the equalities $\lambda_{1f} = \lambda_{2f}$ and $\lambda_{1\theta} = \lambda_{2\theta}$ in the problem formulation (9)–(12) considered in the present paper do not follow from the numerical model. The calculated values of the microscales are results

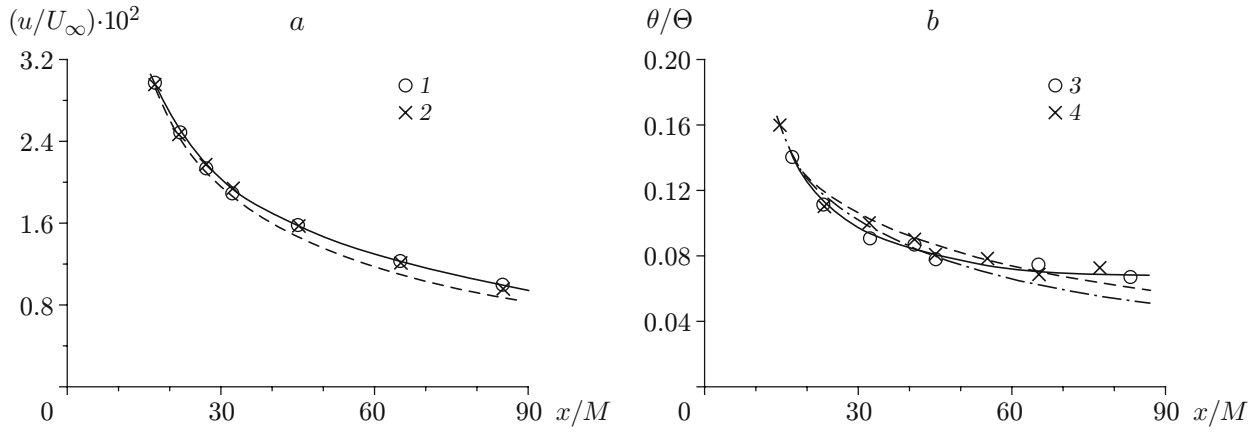

Fig. 3. Quantities u/U_∞ (a) and θ/Θ (b) versus x/M: points 1–4 are the experimental data [10] behind a heated grid (1), behind a cold grid (2), and in different experiments (3 and 4); the solid curves are the results of processing of the experimental data in [10], the dashed curves are the results calculated at $\varkappa_2 = 0.095$, and the dot-and-dashed curve is the results calculated at $\varkappa_2 = 0.125$.

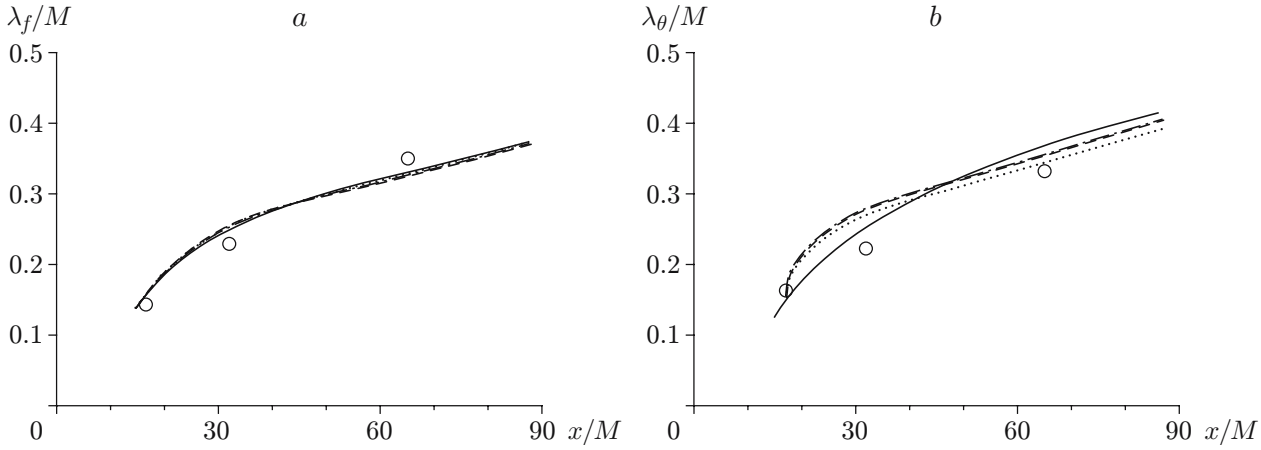

Fig. 4. Taylor microscale λ_f (a) and Corrsin microscale λ_θ (b): the points are the experimental values obtained in [10] for λ_{1f} (a) and $\lambda_{1\theta}$ (b); the solid curves are the results of processing of the experimental data in [10] for λ_{2f} (a) and $\lambda_{2\theta}$ (b); the dashed, dotted, and dot-and-dashed curves are the results calculated in the present work for λ_{1f}, λ_{2f}, and λ_{3f}, respectively (a), and for $\lambda_{1\theta}$, $\lambda_{2\theta}$, and $\lambda_{3\theta}$, respectively (b).

of processing of the data obtained in a numerical experiment (in [10], the data of a laboratory experiment). In the present work, we also considered a modification of the numerical model with the boundary conditions imposed at $r = 0$ instead of the Neumann conditions for the correlation functions [thus, the equality of the microscales determined by Eqs. (13) and (14) was introduced into the model]:

$$\Big(\frac{\partial B_{LL}}{\partial t}\Big)\Big|_{r=0} = \frac{10}{\mathrm{Re}_M}\Big(\frac{\partial^2 B_{LL}}{\partial r^2}\Big)\Big|_{r=0}, \qquad \Big(\frac{\partial B_{\theta\theta}}{\partial t}\Big)\Big|_{r=0} = \frac{6}{\mathrm{Pe}_M}\Big(\frac{\partial^2 B_{\theta\theta}}{\partial r^2}\Big)\Big|_{r=0}. \tag{15}$$

The values of λ_{3f} and $\lambda_{3\theta}$ found thereby are close to the values of λ_{1f}, λ_{2f}, $\lambda_{1\theta}$, and $\lambda_{2\theta}$ (Fig. 4). The effect of the boundary conditions (15) on the calculated values of $B_{LL}(r,t)$ and $B_{\theta\theta}(r,t)$ turns out to be insignificant. The grid values of the correlation functions differ by less than 1% in a uniform grid norm for the entire interval of the values of t considered.

Based on the experimentally found values of $u = \sqrt{B_{LL}(0,t)}$, λ_f, and λ_θ, we calculated the turbulent Reynolds and Peclet numbers $\mathrm{Re}_\lambda = u\lambda_f/\nu$ and $\mathrm{Pe}_\lambda = u\lambda_\theta/\chi$. At $t = x/M = 20$–65, the values of the turbulent Reynolds and Peclet numbers were observed to decrease and to stay in the intervals $\mathrm{Re}_\lambda = 26.1$–$35.6$ and $\mathrm{Pe}_\lambda =$

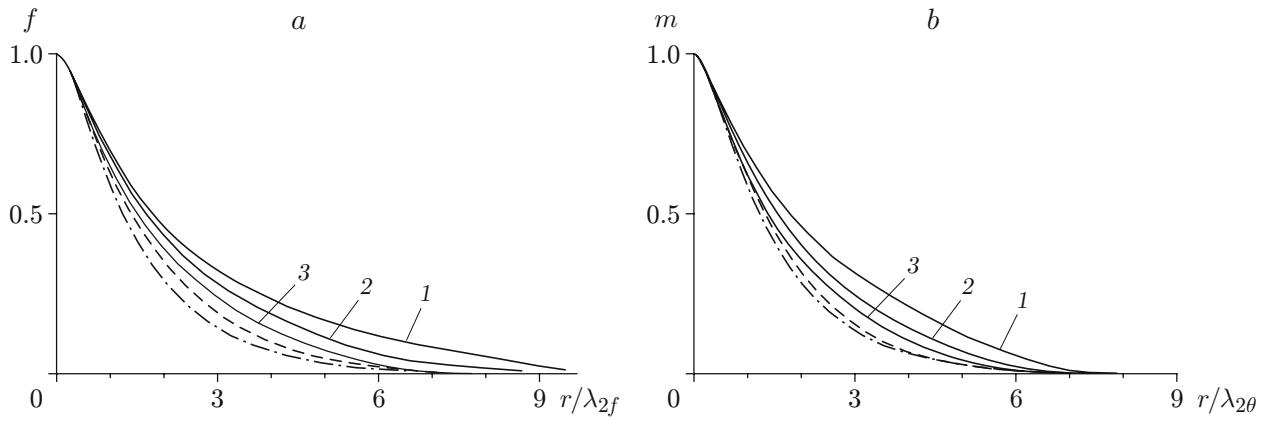

Fig. 5. Calculated and experimental normalized correlation functions: (a) $f(r) = B_{LL}(r,t)/B_{LL}(0,t)$; (b) $m(r) = B_{\theta\theta}(r,t)/B_{\theta\theta}(0,t)$; the solid curves show the experimental data for $x/M = 17$ (1), 32 (2), and 65 (3); the dashed curves are the results calculated at $t = x/M = 32$ and the dot-and-dashed curves are the results calculated at $t = x/M = 65$.

20.3–28.8. These results are consistent with the experimental data [10], which testifies to weak variations of the turbulent Reynolds and Peclet numbers at the initial stage of turbulence degeneration behind the grid. The fact of slow variation of Re_λ was previously noted in [3, 4, 6]. In formulating the closing relations (3) and (4), we noted that the empirical constant $\varkappa_1$ is calculated via the universal Kolmogorov constant C_u corresponding to the presentation of the structural function D_{LL} in the inertial (inertial-convective) interval of scales. The numerical experiments performed (see also [2–6]) show that the quantity $\varkappa_1$ is fairly universal. Concerning the empirical constant $\varkappa_2$, as we noted above, the value $\varkappa_2 = 0.095$ was chosen with allowance for the requirement of matching of the calculated and experimental data [10]. The choice of $\varkappa_2 = \mathrm{const}$ for numerical modeling of the dynamics of turbulent fluctuations of temperature at the initial stage of modeling of turbulence degeneration behind a heated grid in the wind tunnel is caused by small changes Pe_λ (Re_λ) within the interval of distances considered.

Figure 5a shows the calculated and experimental normalized correlation functions $f(r)$. The agreement of the data can be considered as reasonable (other examples with good agreement of the calculated and experimental data can be found in [2–6] and are plotted in Fig. 2).

Figure 5b shows the calculated normalized correlation functions $m(r)$. It is seen that the calculated and measured functions are in reasonable agreement. The results calculated for $\varkappa_2 = 0.125$ (not shown in Fig. 5) are in better agreement with the experimental data. In this case, however, there are significant differences in the calculated and measured values of θ (see Fig. 3b).

In the numerical experiments, we also analyzed the changes in $\Lambda(t) = \int\limits_0^\infty r^4 B_{LL}(r,t)\,dr$ (Loitsyanskii invariant) and $K(t) = \int\limits_0^\infty r^2 B_{\theta\theta}(r,t)\,dr$ (Corrsin invariant). In the numerical solution, the values of these quantities remained constant: $L(t) = 5.235 \cdot 10^{-5}$ and $K(t) = 1.247 \cdot 10^{-3}$. Thus, the calculated results do not contradict the hypothesis about the existence of finite, other than zero, Loitsyanskii and Corrsin invariants [1]. The Loitsyanskii invariant was discussed in detail in [3, 4].

Conclusions. The following basic results were obtained during the activities described above. A numerical model of the dynamics of turbulence and temperature fluctuations behind a heated grid in a wind tunnel, based on the closed Kármán–Howarth and Corrsin equations, was constructed. Reasonable agreement between the calculated results and the experimental data [10] was achieved.

The authors are grateful to V. A. Kostomakha for useful discussions and attention to this work.

This work was supported by the Russian Foundation for Basic Research (Grant Nos. 04-01-00209a and 07-01-00363a), by the Council on the Grants of the President of the Russian Federation on Supporting the Leading

Scientific Schools of the Russian Federation (Grant No. NSh-9886.2006.9), and by the Siberian Division of the Russian Academy of Sciences (Joint Integration Project No. 103 between the Siberian Division of the Russian Academy of Sciences, Far-East Division of the Russian Academy of Sciences, and Ural Division of the Russian Academy of Sciences).

REFERENCES

1. A. S. Monin and A. M. Yaglom, *Statistische Hydromechanik*, Verlag–Nauka, Moskau (1965).
2. V. A. Kostomakha, "Structure of isotropic and locally isotropic turbulence," Candidate's Dissertation in Phys. and Math., Novosibirsk (1986).
3. U. A. Klimentenok, Zh. L. Korobitsyna, and G. G. Chernykh, "Numerical implementation of the Loitsyanskii–Millionshchikov asymptotic solution," *Mat. Model.*, **7**, No. 1, 69–80 (1995).
4. G. G. Chernykh, Z. L. Korobitsina, and V. A. Kostomakha, "Numerical simulation of isotropic turbulence dynamics," *Int. J. Comput. Fluid Dyn.*, **10**, No. 2, 173–182 (1998).
5. Yu. M. Lytkin and G. G. Chernykh, "One method of closing the Kármán–Howarth equation," in: *Dynamics of Continuous Media* (collected scientific papers) [in Russian], No. 27, Inst. Hydrodynamics, Sib. Div., Acad of Sci. of the USSR (1976), pp. 124–130.
6. Yu. M. Lytkin and G. G. Chernykh, "Calculations of correlation functions in isotropic turbulence," in: *Dynamics of Continuous Media* (collected scientific papers) [in Russian], No. 35, Inst. Hydrodynamics, Sib. Div., Acad of Sci. of the USSR (1978), pp. 74–88.
7. M. Oberlack and N. Peters, "Closure of the two-point correlation equation as a basis for Reynolds stress models," *Appl. Sci. Res.*, **51**, 533–538 (1993).
8. A. T. Onufriev, *Description of Turbulent Transport. Nonequilibrium Models: Students' Book*, Moscow Inst. Phys. Technol., Moscow (1995).
9. J. A. Domaradzki and G. L. Mellor, "A simple turbulence closure hypothesis for the triple-velocity correlations functions in homogeneous isotropic turbulence," *J. Fluid Mech.*, **140**, 45–61 (1984).
10. R. R. Mills, A. L. Kistler, V. O'Brien, and S. Corrsin, "Turbulence and temperature fluctuations behind a heated grid," Tech. Note No. 4288, NACA, Washington (1958).
11. Z. Warhaft, "Passive scalars in turbulent flows," *Annu. Rev. Fluid Mech.*, **32**, 203–240 (2000).
12. R. A. Antonia, R. J. Smalley, T. Zhou, et al., "Similarity solution of temperature structure functions in decaying homogeneous isotropic turbulence," *Phys. Rev. E*, **69**, 016305-1–016305-11 (2004).
13. A. T. Onufriev and O. A. Pyrkova, "Problem of weak turbulence decay in a homogeneous flow," Preprint No. 2005-1, Moscow Inst. Phys. Technol., Dolgoprudnyi (2005).
14. R. A. Antonia, T. Zhou, and G. Xu, "Second-order temperature and velocity structure functions: Reynolds number dependence," *Phys. Fluids*, **12**, No. 6, 1509–1517 (2000).
15. A. A. Samarskii, *Introduction into the Theory of Difference Schemes* [in Russian], Nauka, Moscow (1971).